# Nonmetallic left-handed material based on negative-positive anisotropy in low-dimensional quantum structures

Pavel Ginzburg and Meir Orenstein[a)]
*Department of Electrical Engineering, Technion, Haifa 32000, Israel*

(Received 7 February 2008; accepted 11 February 2008; published online 17 April 2008)

Nonmetallic left-handed material by assembly of low-dimensional quantum structures is theoretically proposed. Specifically, we predict relatively wideband, tunable left-handed material by employing structures comprised of semiconductor quantum wells and quantum dots. Well established epitaxial growth of semiconductor material allows a feasible composition of such metamaterials. The advantages of the proposed scheme is the potential ability to invert the material losses to gain by electrical pumping and the possibility to switch the material regime from left-handed to right-handed by applying external voltage, which are not affordable in the recently proposed left-handed material configurations. © *2008 American Institute of Physics*. [DOI: 10.1063/1.2906183]

## I. INTRODUCTION

Left-handed materials (LHMs) are artificially assembled effective media, with a predominant feature of exhibiting negative index of refraction.[1] The aspiration is that their peculiar properties will lead to superior imaging[2] and may provide the avenue to observe "negative analogies" of important optical phenomena, such as the Doppler shift and Cerenkov radiation.[1] Most of LHM metamaterials designed for the visible–near infrared (IR) spectrum are based on metal inclusions, thus they are accompanied by high energy loss which limits their applicability (Refs. 3–7 and overview in Ref. 8). Here we propose a concept of metamaterial assembly where metal inclusions are replaced by semiconductor based low-dimensional quantum structures, exhibiting significantly lower losses and even may be inverted to exhibit gain by carriers' injection. Only very few theoretical realizations of nonmetallic optical LHM were proposed: gaseous nonmetallic LHM (Refs. 9–11) which employs a quantum interference technique[12] (EIT) and requires high density gas and exhibiting by ultranarrow frequency range of the LHM properties. A chiral LHM material was proposed by Pendry[13] and recently theoretically projected in general quantum system.[14] The metal inclusion based LHM not only suffers from high losses but also requires extreme nanoprocessing. The scheme proposed in this paper is using the well established technology of epitaxial growth. We predict relatively wideband LHM (compared to Refs. 9–11) by employing structures comprised of semiconductor quantum wells[15] (QWs) and quantum dots[16] (QDs). One of the most important advantages of the proposed scheme is the potential ability to invert the resonance from absorption to gain—a virtue that cannot be realized in metals.

To emphasize we are not using the free carrier plasma of semiconductors[17] or its optical phonons interaction[18] which may yield a negative dielectric constant in the far IR, but rather the permittivity due to transition resonances between subbands of the semiconductor low dimensionality quantum structure.

## II. LHM BY QUANTUM SYSTEM ANISOTROPY

We start from a configuration recently proposed in Ref. 4 and further developed in Ref. 19, where the negative $\mu$ ingredient of the negative index is replaced by an exceptionally high anisotropic waveguide structure. Some of the transverse magnetic (TM) optical modes, propagating within a waveguide with positive-negative anisotropic core, will be effectively left handed. We look into two possible structures consisting of either QWs or coupled QDs to achieve the required anisotropy ($\varepsilon_{\perp}<0$ and $\varepsilon_{\parallel}>0$) and thus to implement a LHM. The waveguide core will contain the layered QWs [Fig. 1(a)] or vertically grown aligned QDs stack [Fig. 1(b)]. The anisotropy in our scheme originates from the difference between the in plane and vertical (growth direction) susceptibility of the quantum structure for the intersubband transitions, namely, dipolar selection rules for QWs and polarization dependent tunnelling efficiency for coupled QDs. Although the pronounced effects are in the vicinity of transition resonances, lower loss relatively to metal based metamaterials is expected. Additional merit of the quantum structure, not mentioned in the introduction, is a tuning capability [e.g., from LHM to right-handed material (RHM)], by applying voltage on the structure, and probably the most outstanding feature (gain by carrier injection is possible for semiconductor LHM realizations using quantum cascade amplifier configurations Refs. 20 and 21).

## III. MATERIALS FOR LHM COMPOSITION

We believe that the material of choice for dispersion engineering in the visible–near IR regime is the relatively novel nitride alloys family[22]—actually InN/GaN/AlN QWs/QDs.[16,23] This material family exhibits a large conduction band (CB) offsets and wide energy gap, enabling near IR and visible range interactions via intersubband transitions. In

[a)]Electronic mail: meiro@ee.technion.ac.il.

 

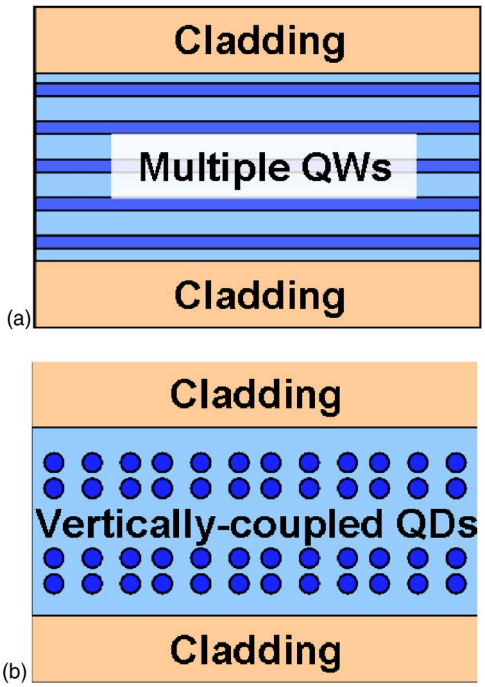


FIG. 1. (Color online) Slab waveguides with anisotropic core composed of low-dimensional quantum structures. Anisotropy comes from spatial composition of embedded structures and leads to LHM properties (Ref. 4): (a) core composed of quantum wells; (b) core composed of coupled quantum dots.

addition, the Fermi level in such nitride composite can be located within the CB which allows the passive employment of such structures (without prepopulation by electrical pump or doping). Furthermore this material has a relatively low background dielectric constant which facilitates the approach to the negative zone. However, since the nitride compound semiconductors are relatively young nor their growth is perfected yet, neither all their spectroscopic data is available. Thus we deliberately dwell here both on the nitride family and on the well established GaAs/AlGaAs heterostructure to provide the proof of concept of the proposed mechanism. A detailed study of nitride system exhibiting both negative-positive anisotropy as well as gain is reported elsewhere.[24] The GaAs/AlGaAs and InGaAs/AlInAs composites used for infrared detectors and quantum cascade lasers exhibit their intersubband optical transitions in the IR region.

## IV. QW BASED LHM

The origin of optical permittivity tensor anisotropy [Eq. (1)] in QWs is the polarization dependent dipole matrix element for intersubband transitions. The light beam being polarized in the plane of the QWs growth will strongly interact with the resonant CB electron, while the polarization perpendicular to the growth direction will not be affected by the QW.

$$\varepsilon = \begin{pmatrix} \varepsilon_\perp & 0 & 0 \\ 0 & \varepsilon_\parallel & 0 \\ 0 & 0 & \varepsilon_\parallel \end{pmatrix}, \quad \varepsilon_\parallel = \varepsilon_{\text{back}} > 0, \quad \varepsilon_\perp < 0. \tag{1}$$

The intersubband induced permittivity can be represented by Lorenzian model[25] as follows:

$$\varepsilon_\perp = \varepsilon_{\text{bak}} - iNq\frac{|\mu_{12}|^2(\rho_{11}-\rho_{22})}{\varepsilon_0\hbar}\frac{1}{i(\omega-\omega_{21})-\gamma_{21}}\Gamma, \tag{2}$$

where $q$ is the electron charge, $\varepsilon_0$ is the vacuum electric permittivity, $\omega_{12}$ is the resonant intersubband transition frequency, $\omega$ is the central frequency of the input light, $\rho_{ii}$ is the electron occupation density of the $i$th level (reduced to the ground state for passive device and to the exited for active), $N$ is the density of carriers (participating in the process), $\varepsilon_{\text{bac}}$ is the averaged permittivity of the background material, $\gamma_{21}$ is the phenomenology introduced dephasing rate, and $\Gamma$ is the optical field confinement factor within the well layer. Theoretically, by choosing the appropriate parameters, it is possible to reach the negative real part of $\varepsilon$ in the vicinity of a resonance, but practically there are number of obstacles to mitigate. The first is achieving a sufficiently high electron density by strong electrical pump or by doping of the QW layer; nevertheless the electron population still will be limited by $\sim 10^{19}$ cm$^{-3}$ due to recombination processes. The outstanding advantage of the nitrides is the location of the room temperature Fermi level, within the CB which is contributing to very high electron population (up to the Avogadro number!).

The other crucial parameter is the dephasing. The dephasing rate is in general a consequence of several physical processes. The most significant contributors are interface roughness scattering, phonon scattering, impurity scattering, alloys disorders, many-body effects (electron-electron, electron-hole scattering[26]), and subband dispersion.[27] While the phonon scattering may be significantly reduced by temperature manipulation, a further reduction of the dephasing rate is limited by technology issues[26] as well as the intrinsic material structure.[27] The nowadays dephasing values (linewidth) are few meV for cryogenic QWs and tens of meV for room temperature devices.

The last factor contributing to the optical permittivity is the field confinement $\Gamma$ [Eq. (2)], which is relatively small in conventional structures, e.g., semiconductor lasers or superlattices explored in spectroscopy. This is the reason why very deep resonances were measured but yet without demonstrating a negative dielectric response.[28] The very recent work of Frogley *et al.*[29] exhibiting negative resonances in a semiconductor inversionless laser, removes the doubts that negative $\varepsilon$ can be achieved in the vicinity of QW intersubband resonance.

We explore a GaAs/$Al_{0.3}Ga_{0.7}As$ structure to demonstrate a medium exhibiting a negative $\varepsilon$. Many other variants of material families will exhibit the same phenomena and can be optimally engineered for applicable devices. The parameters for GaAs/$Al_{0.3}Ga_{0.7}As$ QW were taken from experimental data[25] as follows: well depth $\Delta E_c = 230$ meV, well width $L = 10$ nm, and the volume density of charge of $1 \times 10^{18}$ cm$^{-3}$. Dephasing rate of the dipolar transitions was chosen to be $\gamma_{12} = 3$ meV.[26] $\varepsilon_{\text{back}}$ is the average between the constituents and its value is $\sim 13$. The waveguide core is designed to contain about 30% QW layers. The simulation considers a simple model of density matrix approach,[25] ignoring the many-body effects, such as carrier screening, scattering processes, band gap renormalization, and Coulomb

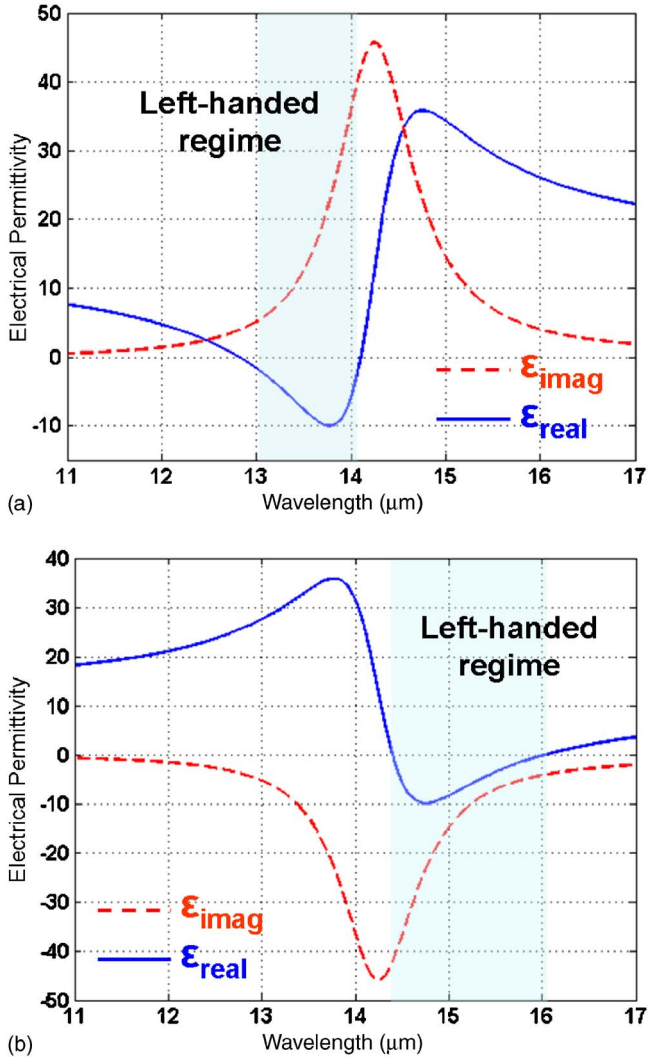


FIG. 2. (Color online) The criterion for LHM operation is that the perpendicular term of electrical permittivity tensor of the waveguide core is negative and its parallel term is positive (Ref. 4). While the parallel part is always positive, the perpendicular part of permittivity tensor of the waveguide core based on QW inclusions is depicted. Transparent bar highlights the LHM region: (a) passive device; (b) active device.

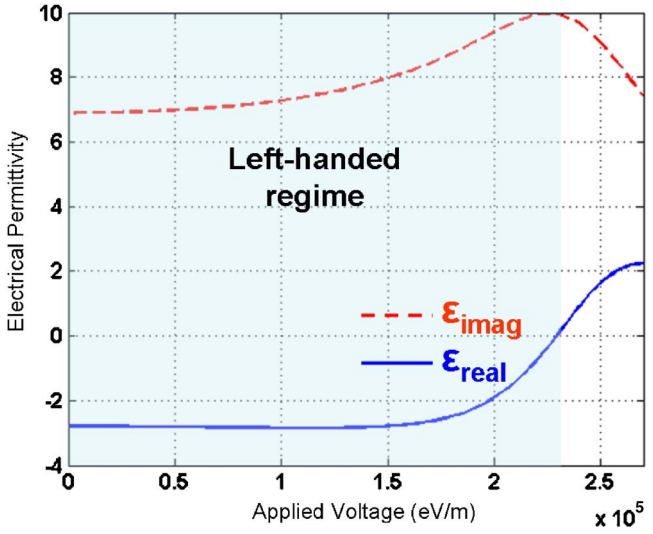


FIG. 3. (Color online) The considerable advantage of semiconductor devices is their sensitivity to applied voltage. This external trigger changes the configuration of internal quantum levels, leading the voltage controllability of material regime. Transparent bar highlights the LHM region.

enhancement,[30,31] which play a significant role for fine device design but may be neglected for zero order approximation. We also neglect the free carrier absorption losses that are small compared to the resonant transition loss. The results depicted in Fig. 2(a) exhibit evident negative dielectric resonance in the far IR range. Choosing the wavelength of operation as 13 $\mu$m, we obtain the $\varepsilon_{\perp}=-1.56+5.22j$, while $\varepsilon_{\parallel}=13$. For a 13 $\mu$m thick slab embedded in perfectly conducting layers (configuration of Ref. 4), the effective refractive index for the fourth TM mode is $-0.9+0.6j$, and for a more realistic situation, namely, a slab in the air[19] the fifth TM mode has an effective refractive index of $-2.1+1.6j$. The figure of merit (ratio of real to imaginary) is more than 1, which is better than most of what is achieved from metals (e.g., the reported results in Refs. 7) and approaching the best recently reported by Dolling *et al.* in Ref. 32, and may be further improved at cryogenic temperature or by using other material alloys.

Additional significant feature of the proposed configuration is its controllability. The control is achieved by coupling QWs and applying an inverse bias voltage on them to determine the coupling coefficient which is a dominant factor in the magnitude of the susceptibility. By this control switching the material from LHM to RHM regime is achieved, and more details for such a configuration can be found in Ref. 33. Exploiting this concept, in Fig. 3 we depict the switching between LHM and RHM regimes by voltage control of the $\varepsilon_{\perp}$ sign. For zero bias, the $\varepsilon$ value is negative at the prescribed wavelength, while for a large bias the coupled QWs move out resonance and the permittivity shifts to the positive RHM regime. Furthermore, introducing a structure of multiple coupled wells, namely, a QWs superlattice, not only enhances the confinement factor of the optical mode but significantly increases the bandwidth of the device.[34]

A prominent advantage of semiconductors over metals is a possibility to convert the loss to gain by electrical current pump, inverting the population, while preserving the previously discussed positive negative anisotropy. For the intersubband transitions the configuration of an active region of a quantum cascade laser (QCL) will serve as the gain LHM slab. Actually $\varepsilon$ of Eq. (2) is still valid when replacing the expression $\rho_{11}-\rho_{22}\approx 1$ to be $\rho_{11}-\rho_{22}\approx -1$ (complete population inversion). This can be achieved in a conventional QCL by introducing additional (third) energy level with fast nonradiative transition rate and further tunnelling to the next cascade level. Under the same discussed constrains and injecting electron current, an active LHM may be achieved [Fig. 2(b)]. The resulting parameters are $\varepsilon_{\perp}=-9.9-24.5j$ and $\varepsilon_{\parallel}=13$, leading to a refractive index of $-3.4-2.3j$ for 13 $\mu$m slab embedded in perfectly conducting layers. The fourth TM mode of such a slab in air[19] has an effective index of $-2-1.47j$. A detailed design of a related negative $\varepsilon$+gain in the nitride family is reported in Ref. 24, although the design requires gain factors not achievable yet by current technologies.

The realization of the proposed QWs based on aniso-

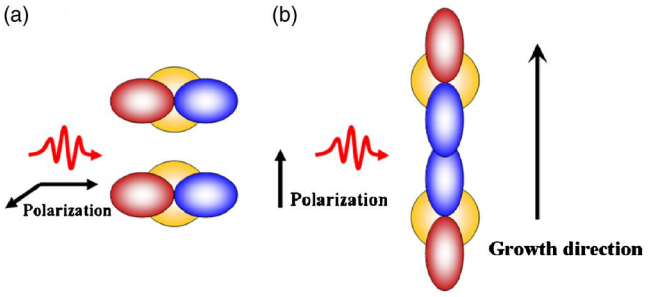


FIG. 4. (Color online) Schematics of metamaterial comprised of coupled QDs. The required anisotropy (Ref. 4) comes from spatial organization of QDs. Dipole selection rules define the orientation of the $p$ orbital of spherical QD. Horizontally polarized incident light (a) encounters negligibly coupled QDs, while vertical polarization (b) interacts with highly coupled structure.

tropic slab waveguide is quite straight forward by nowadays technology. However, significant losses still exist in the passive configuration. Thus we propose theoretically a passive device based on QDs with significantly reduced losses. The usage of QDs is more promising because the three-dimensional carrier confinement reduces the dephasing rates.[35] Self-assembled QDs (Ref. 16) has a substantial size distribution resulting in an inhomogeneous line broadening,[36] which may currently prevent the implementation of the LHM. However, controlled growth of ordered QDs is now under intense research effort[37] and hopefully will mitigate the broadening deficiency of the QDS based LHM.

## V. QD BASED LHM

The QD based LHM is based on the strong anisotropy with negative resonances of pairs of vertically coupled InN/AlN QDs.[38] For simplicity of the numerical calculation we assume spherical QDs, but the existing hexagonal-pyramidal InN/AlN QDs (Ref. 16) will lead to similar results. It should be noted that realistic (nonspherical) singular QDs are by themselves anisotropic structures[39] but we decided to exploit the coupled QDs configuration to enhance the anisotropy as well as to achieve controllability as discussed in the previous section. Coupled pairs of 3 nm diameter QDs can be prepared by growing two layers of aligned QDs, separated by 5 nm. We select the spacing between the dots to provide a finite tunnelling[38] for the excited states ($p$ states) while negligible for the ground state ($s$ state) (explicit calculations yield a coupling ratio of ~53). The Fermi level crossing the CB manifests the electron occupation of the s-shaped ground state. The "bonding" due to the exited states coupling depends on the angular functions due to conservation of the angular momentum in a resonant tunnelling process.[40] In Fig. 4 the coupling of the wave functions with angular momentum along [Fig. 4(a)] or transverse [Fig. 4(b)] to the molecular axis (growth direction) is shown schematically and provides an intuitive explanation for the origin of anisotropy. The explicit calculations give a ratio of ~15.4 between the respective coupling constants. The detailed treatment of such four-level system may be found in Ref. 33. Envelope wave functions of layered structure (QW) should

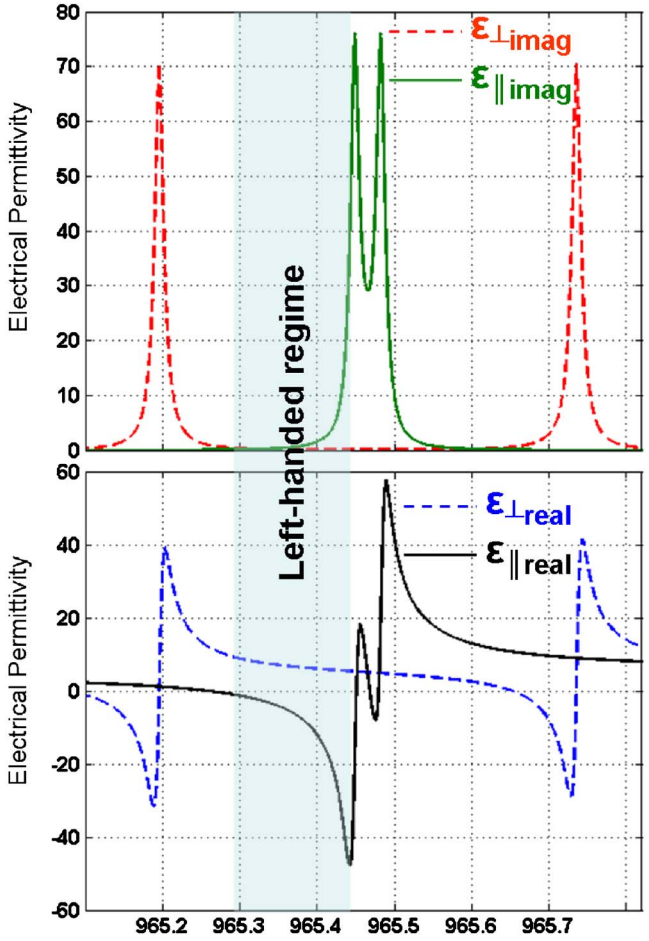


FIG. 5. (Color online) Simulation of imaginary (top) and real (bottom) parts of electric permittivity of the system of coupled QDs. The electric permittivity curves represent the anisotropy of the $\varepsilon$ tensor. Transparent bar highlights the Podolskiy-Narimanov criterion ($\varepsilon_\perp<0$ and $\varepsilon_\parallel>0$) hence, the region of LHM.

be replaced by hydrogen like spherical potential.[41] Strong anisotropy is not enough for realizing LHM. The medium should exhibit also negative horizontal and positive vertical $\varepsilon$ values. In order to address this point we performed simulations of a layered structure comprised of coupled QDs using the following material parameters: $\Delta E_c=3.65$ eV, $m_{\mathrm{InN}}=0.07m_0$, $m_{\mathrm{AlN}}=0.32m_0$, $\lambda_{\mathrm{central}}=965.5$ nm, $\gamma=7$ $\mu$eV, and dots density $N=4\times10^{23}$ m$^{-3}$. In the region indicated by an arrow in Fig. 5, the Podolskiy-Narimanov criterion[4] $\varepsilon_\perp<0$ and $\varepsilon_\parallel>0$ is fulfilled. The resulting values for electrical permittivity at $\lambda=956.3$ nm, the wavelength of minimal loss, are $\varepsilon_\perp=-3.5+0.2j$ and $\varepsilon_\parallel=7.4+0.2j$. The resulting refractive index is $-5+0.01j$ for the sixth order mode of 1 $\mu$m slab in the configuration of Ref. 4. Here, the theoretical figure of merit is even better than the best recently reported experiment.[32]

## VI. CONCLUSIONS

In conclusion we proposed the usage of low-dimensional quantum system for LHM implementation. Two different schemes have been proposed: QWs and coupled QDs based anisotropic waveguides. A comparable or even reduced loss compared to the currently discussed LHM is estimated. Two

significant features of tunability and gain, missing in metal based implementations, are possible in our configuration. In addition, a fast development of the nitride group materials shows a remarkable promise for realization of our proposition for visible light.


[1]V. G. Veselago, Sov. Phys. Usp. **10**, 509 (1968).
[2]J. B. Pendry, Phys. Rev. Lett. **85**, 3966 (2000).
[3]V. M. Shalaev, W. Cai, U. K. Chettiar, H. -K. Yuan, A. K. Sarychev, V. P. Drachev, and A. V. Kildishev, Opt. Lett. **30**, 3356 (2005).
[4]V. A. Podolskiy and E. E. Narimanov, Phys. Rev. B **71**, 201101(R) (2005).
[5]L. V. Panina, A. N. Grigorenko, and D. P. Makhnovskiy, Phys. Rev. B **66**, 155411 (2002).
[6]T. J. Yen, W. J. Padilla, N. Fang, D. C. Vier, D. R. Smith, J. B. Pendry, D. N. Basov, and X. Zhang, Science **303**, 1494 (2004).
[7]A. N. Grigorenko, A. K. Geim, H. F. Gleeson, Y. Zhang, A. A. Firsov, I. Y. Khrushchev, and J. Petrovic, Nature (London) **438**, 335 (2005).
[8]C. M. Soukoulis, S. Linden, and M. Wegener, Science **315**, 47 (2007).
[9]M. Ö. Oktel and Ö. E. Müstecaplioglu, Phys. Rev. A **70**, 053806 (2004).
[10]Q. Thommen and P. Mandel, Phys. Rev. Lett. **96**, 053601 (2006).
[11]S. Jian-qi, R. Zhi-chao, and H. Sai-ling, COMSAT Tech. Rev. **5**, 1322 (2004).
[12]S. E. Harris, Phys. Today **50**(7), 36 (1997).
[13]J. B. Pendry, Science **306**, 1353 (2004).
[14]J. Kästel, M. Fleischhauer, S. F. Yelin, and R. L. Walsworth, Phys. Rev. Lett. **99**, 073602 (2007).
[15]S. Ochi, N. Hayafuji, Y. Kajikawa, K. Mizuguchi, and T. Murotani, J. Cryst. Growth **77**, 553 (1986).
[16]S. Ruffenach, B. Maleyre, O. Briot, and B. Gil, Phys. Status Solidi C **2**, 826 (2005).
[17]A. J. Hoffman, L. Alekseyev, S. S. Howard, K. J. Franz, D. Wasserman, V. A. Podolskiy, E. E. Narimanov, D. L. Sivco, and C. Gmach, Nat. Mater. **6**, 946 (2007).
[18]D. Korobkin, Y. Urzhumov, and G. Shvets, J. Opt. Soc. Am. B **23**, 468 (2006).
[19]Y. Satubi, N. Kaminski, and M. Orenstein, J. Opt. Soc. Am. B **24**, A62 (2007).
[20]J. Faist, F. Capasso, D. L. Sivco, C. Sirtori, A. L. Hutchinson, and A. Y. Cho, Science **264**, 553 (1994).
[21]C. Sirtori, P. Kruck, S. Barbieri, P. Collot, J. Nagle, M. Beck, J. Faist, and U. Oesterle, Appl. Phys. Lett. **73**, 3486 (1998).
[22]B. Monemar and G. Pozina, Prog. Quantum Electron. **24**, 239 (2000).
[23]M. G. Cheong, E. K. Suh, and H. L. Lee, Semicond. Sci. Technol. **16**, 783 (2001).
[24]P. Ginzburg and M. Orenstein, Conference of Lasers and Electro-Optics CLEO, Baltimore, 10 May 2007 (unpublished), http://arxiv.org/abs/0707.0097
[25]P. Basu, *Theory of Optical Processes in Semiconductors: Bulk and Microstructures* (Clarendon, Oxford, 1997).
[26]K. L. Campman, H. Schmidt, A. Imamoglu, and A. C. Gossard, Appl. Phys. Lett. **69**, 2554 (1996).
[27]I. Waldmüller, M. Woerner, J. Förstner, and A. Knorr, Phys. Status Solidi B **238**, 474 (2003).
[28]K. Unterrainera, R. Kersting, R. Bratschitsch, G. Strasser, J. N. Heyman, K. D. Maranowski, and A. C. Gossard, Physica E (Amsterdam) **7**, 693 (2000).
[29]M. D. Frogley, J. F. Dynes, M. Beck, J. Faist, and C. C. Phillips, Nat. Mater. **5**, 175 (2006).
[30]W. W. Chow, S. W. Koch, and M. Sargent III, *Semiconductor-Laser Physics* (Springer, Berlin, 1994).
[31]C. F. Hsu, P. S. Zory, C. H. Wu, and M. A. Emanuel, IEEE J. Sel. Top. Quantum Electron. **3**, 158 (1997).
[32]G. Dolling, C. Enkrich, M. Wegener, C. M. Soukoulis, and S. Linden, Opt. Lett. **31**, 1800 (2006).
[33]P. Ginzburg and M. Orenstein, Opt. Express **14**, 12467 (2006).
[34]P. Ginzburg and M. Orenstein, *Photonic Metamaterials: From Random to Periodic on CD-ROM* (The Optical Society of America, Washington, DC, 2006).
[35]N. H. Bonadeo, J. Erland, D. Gammon, D. Park, D. S. Katzer, and D. G. Steel, Science **282**, 1473 (1998).
[36]J. Misiewicz, G. SImagek, and K. Ryczko, Curr. Appl. Phys. **3**, 417 (2003).
[37]Z. Zhong, J. Novak, J. Stangl, T. Fromherz, F. Schäffler, and G. Bauer, J. Phys.: Conf. Ser. **38**, 69 (2006).
[38]E. A. Stinaff, M. Scheibner, A. S. Bracker, I. V. Ponomarev, V. L. Korenev, M. E. Ware, M. F. Doty, T. L. Reinecke, and D. Gammon, Science **311**, 636 (2006).
[39]M. Sugisaki, H. Ren, S. V. Nair, K. Nishi, S. Sugou, T. Okuno, and Y. Masumoto, Phys. Rev. B **59**, R5300 (1999).
[40]U. Gennser, M. Scheinert, L. Diehl, S. Tsujino, A. Borak, C. V. Falub, D. Grützmacher, A. Weber, D. K. Maude, G. Scalari, Y. Campidelli, O. Kermarrec, and D. Bensahe, Europhys. Lett. **74**, 882 (2006).
[41]C. Cohen-Tannoudji, *Quantum Mechanics* (Wiley-Interscience, New York, 1977).